ISSN 1063-7710, Acoustical Physics, 2012, Vol. 58, No. 6, pp. 713–717. © Pleiades Publishing, Ltd., 2012.

ACOUSTICS OF STRUCTURALLY INHOMOGENEOUS SOLID BODIES. GEOLOGICAL ACOUSTICS

Method for Monitoring Slow Dynamics Recovery[1]

Kristian C. E. Haller and Claes M. Hedberg

Blekinge Institute of Technology, Karlskrona, 37179 Sweden

Abstract—Slow Dynamics is a specific material property, which for example is connected to the degree of damage. It is therefore of importance to be able to attain proper measurements of it. Usually it has been monitored by acoustic resonance methods which have very high sensitivity as such. However, because the acoustic wave is acting both as conditioner and as probe, the measurement is affecting the result which leads to a mixing of the fast nonlinear response to the excitation and the slow dynamics material recovery. In this article a method is introduced which, for the first time, removes the fast dynamics from the process and allows the behavior of the slow dynamics to be monitored by itself. The new method has the ability to measure at the shortest possible recovery times, and at very small conditioning strains. For the lowest strains the sound speed increases with strain, while at higher strains a linear decreasing dependence is observed. This is the first method and test that has been able to monitor the true material state recovery process.

Keywords: material properties, acoustical monitoring, slow dynamics material recovery

DOI: 10.1134/S1063771012060061

Materials with internal cracks or dislocations has a certain type of slow recovery towards equilibrium after a disturbance of its thermodynamic state. This concept is called *Slow Dynamics* (*SD*) which is a reversible process accompanied by nonlinearity [1–9]. In a solid material the slow dynamics is connected to the presence of cracks and dislocations. It can be utilized to determine a material's quality or its damage level. It is an actual material property, and it is therefore important that it can be quantified. A measurement which only measures the *SD* is needed, and this is what is provided in this article.

One effect of the presence of Slow Dynamics is that a disturbance will decrease the material sound speed, evidenced by an immediate shift of the acoustic resonance peak to a lower value [10]. The peak will then slowly recover towards its equilibrium value. Any reaction to a new disturbance on the material before having reached equilibrium will depend on the current state. This means that the material state is dependent on its time history.

An advantage of resonance methods is that they have in general a very high sensitivity. The commonly used acoustic test is a frequency sweep with a constant input force with the frequency being changed step by step. It monitors the maxima of the wave responses indicating the resonant frequencies from which the sound speed of the material can be obtained. A threshold between different strain level regions has been observed. Below it the behavior can be described only by regular Nonlinearity, while above it also non-equilibrium Slow Dynamics occur [6, 11, 12]. This method is here called method A. When the frequency changes in the constant input force sweep, the actual amplitude *inside* the object varies. It is not unusual for factors of 100–1000 to appear, where the maxima are found at the resonant modes' eigenfrequencies. Therefore the material is affected by the strain history, and due to the Slow Dynamics the material is constantly both in a state of recovery and influenced by the time dependent excitation.

It would be better if one could either: B—measure the fast non-linear response while being able to ignore the time history (the Slow Dynamics); or C—measure only the Slow Dynamics while being able to ignore the influence of any fast non-linear dynamics. Method B was presented in [13], and method C is presented in this article.

When the nonlinear responses are accompanied by the Slow Dynamics non-equilibrium recovery, it is difficult to interpret the results and to fit the results to theories. The first method (here called B) which to a significant degree managed to separate the two influences was reported in an earlier Letter [13], where a constant strain resonance frequency test measured the nonlinearity at a minimum of Slow Dynamics. There, the measurements (probing) of the sound velocity were made at the same strain level as the conditioning, followed by another sound velocity measurement at a constant low strain amplitude. There was a time delay on the order of minutes between the conditioning and the low strain measurements during which the material had time to recover. The material state was constant during each of the different strain levels, but the state was by necessity different for each level. These were measurements of the pure nonlinear distortion,

[1] The article is published in the original.

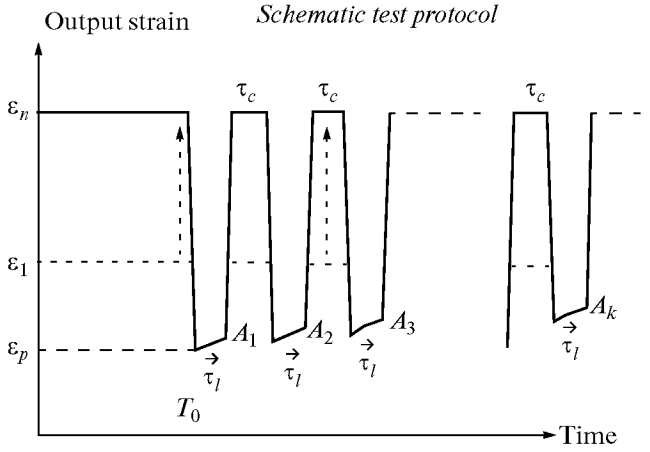

Fig. 1. Details of the test protocol. The probe strain level input ϵ_{Pi} is the same for every cycle resulting in a varying output. The measurement points $A_k \equiv A(\epsilon_n, f_0 + k\Delta f\tau)$ are taken at the five $\tau = \tau_{[1,2,3,4,5]} = [0.2, 0.5, 1, 2, 5]$ seconds for every conditioning level ϵ_n and for every frequency $f_k = f_0 + k\Delta f$. The result are the amplitudes $A(\epsilon_n, f_k, \tau_l)$. T_0 is the 30 minutes during which the conditioning is on before the start of the measurements.

where the otherwise omnipresent non-equilibrium slow dynamics had been minimized. Method B is described thoroughly in [13] where also a comparison between methods A and B is found. The advantage of method B was that the nonlinearity was measured without any *SD* influence, but its disadvantage was that the protocol was slow and it took minutes after the end of conditioning before the actual nonlinearity was recorded.

In this article is described a third method denoted C, which, as an inverted method B, measures the Slow Dynamics without presence of nonlinearity. It is characterized by that the probing wave amplitude is always at a very low strain level, where the nonlinear effects are very weak. On top of that, the nonlinear effect is

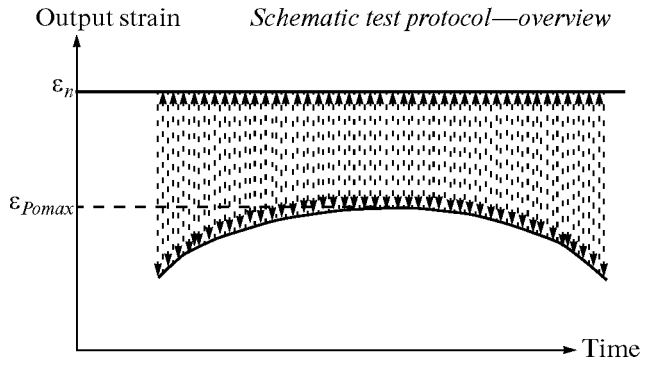

Fig. 2. The schematic protocol for conditioning level ϵ_n. The probe strain level input ϵ_{Pi} is the same for every cycle resulting in a varying output $\epsilon_{Po} \equiv A$ similar to a normal frequency sweep. The lower curve has a maximum $\epsilon_{max}(\epsilon_n, f, \tau) = e(\epsilon_n, f_r, \tau)$ which defines the resonance frequency f_r

also *constant* for all data points, which means that even that small effect is cancelled out because the measurements are comparative.

The novel test protocol that measures the acoustical response at a low probing strain right after being exposed to a high strain conditioning is shown in Figs. 1 and 2 and will now be described in detail. In order to set the object in the specific state related to the conditioning strain level, it is first conditioned for 30 minutes by an acoustic wave at frequency f_{c1} and a drive amplitude a_{c1} corresponding to a strain level ϵ_1. The equivalent resonance frequency for this steady state strain level is $f_c(\epsilon_1)$, which in this article is the same as the conditioning frequency f_{c1}. (To provide for a faster return to equilibrium for every conditioning set, all the used resonance frequencies were determined in advance.) The strain is thereafter changed to a lower strain wave which has a constant low input voltage—the *probe* wave—at a specific frequency f_0 and amplitude a_0. The response amplitude in the object $A(\epsilon_1, f_0, \tau_1) \equiv A(\epsilon_1, f_0, \tau_1)$ is recorded at the time $\tau_1 = 0.2$ seconds. Then the conditioning wave is put back on, at the same strain (ϵ_1) and at the same frequency (f_{c1}) as before, for $\tau_c = 5$ seconds. The conditioning brings the material back to the same state (more or less) irrespective of that the recovery times τ are of different length because conditioning is much faster than recovery. The low amplitude probe wave is moved in frequency to $f_0 + \Delta f$ and the response is recorded as the value $A(\epsilon_1, f_1 = f_0 + \Delta f, \tau_1)$. This frequency sweep process continues for several frequencies $f_k = f_0 + k\Delta f$, each yielding points to the response curve $A(f, \tau_1)$. It will have a maximum value at the resonance frequency $f_r(\epsilon_1, \tau_1)$, which is the first point that goes into the resulting plot. For example, in the sche-

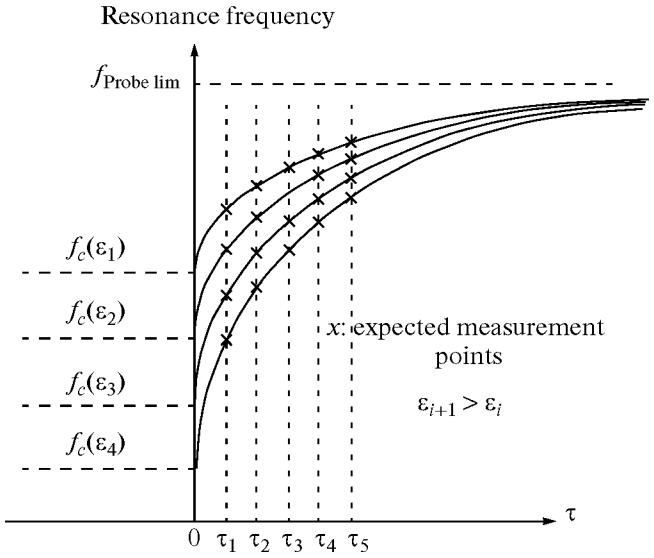

Fig. 3. A schematic plot of expected test results. The time τ is zero when the conditioning wave input ceases.

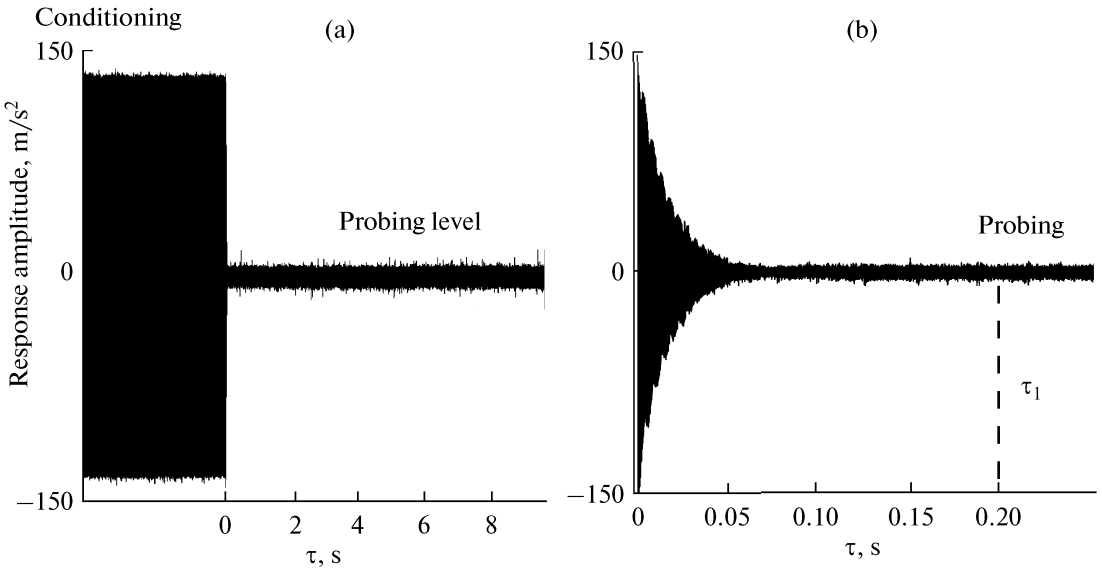

Fig. 4. In (a) the time signal for determination of the delay value τ. In (b) a zoom of the area when switching from conditioning to probing. The input is a swept sine 100 ms 5000–5100 Hz. The conditioning amplitude is here 400 mV and the probing is at 10 mV.

matic plot based on expected results in Fig. 3, this is the upper-left point.

The preceding part is then repeated for the other four probe times τ_l ($l = 2, 3, 4, 5$) = [0.2, 0.5, 1, 2, 5] seconds. This yield the responses $A(\epsilon_1, f_1 = f_0 + \Delta f, \tau_l)$, which will have maxima values at five resonance frequencies $f_r(\epsilon_1, \tau_l)$. These form the first curve that goes into the plots (the upper-most curve in the schematic plot (Fig. 3)).

After this, the complete procedure this far is repeated for the higher conditioning strains ϵ_2, ϵ_3, ..., ϵ_n, ... ϵ_N resulting in N curves, each based on five points.

These measurements are showing the response for times as small as possible, at the beginning of the recovery, which leads to a more accurate frequency recovery, both for earlier times and for lower strains. To measure exactly when the conditioning wave is turned off is not suitable, because it takes time for the interior wave to ring down. For the granite bar in this work the longest ring down time is on the order of 0.1 s, see Fig. 4. Therefore the shortest time τ_1 was chosen to be 0.2 s—at which point the response signal was stable and reliable.

The test object in this article was a granite rock bar, 420 mm long and 50 mm in diameter and the test configuration is shown in Fig. 5.

A continuous sinusoidal acoustical wave was generated at one end of the granite bar by a glued Ferroperm Piezoceramics PZ 26 circular piezo-ceramic with diameter 30 mm and thickness 2.5 mm. A piece of brass was attached to the transducer as a backload. The electrical signal was generated from an Agilent 33250A signal generator and amplified by a Krohn-Hite 7500 amplifier. To match the electric load, a Krohn-Hite MT75R impedance matcher was used. A PCB 352C22 accelerometer picked up the wave and the signal was processed in a Stanford Research SRS830 lock-in amplifier. The granite bar was hanging in a climate chamber in fishing wires to create a free-free boundary condition. Before the measurements started the rock was hanging in the climate chamber for two weeks at test conditions of 20 ± 0.05°C and relative humidity 50 ± 0.1% to reach test condition equilibrium.

In our measurement the number of conditioning strains N is 23. Each starts with 30 minutes at the new conditioning strain for the material to adjust, before the probe measurements begin. This protocol makes it possible to compare the material at different conditioned states—with the *same* probe wave measure-

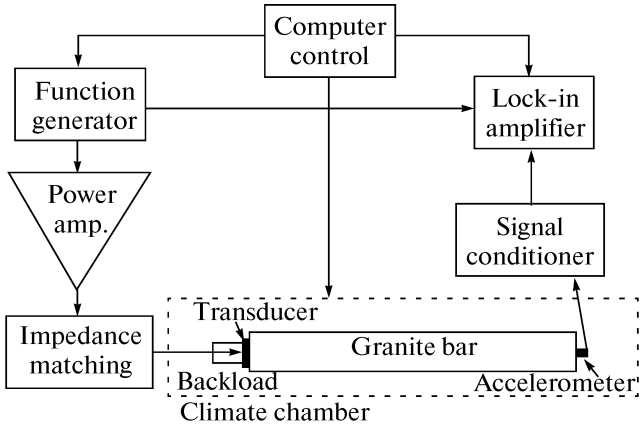

Fig. 5. The test configuration.

The conditioning strains and their curve numbers

6.7×10^{-10} **(1)**	3.3×10^{-8} **(7)**	6.2×10^{-8} **(13)**	3.3×10^{-7} **(19)**
1.6×10^{-9} **(2)**	4.6×10^{-8} **(8)**	1.3×10^{-7} **(14)**	3.4×10^{-7} **(20)**
3.3×10^{-9} **(3)**	4.9×10^{-8} **(9)**	1.9×10^{-7} **(15)**	3.5×10^{-7} **(21)**
6.1×10^{-9} **(4)**	5.3×10^{-8} **(10)**	2.5×10^{-7} **(16)**	4.0×10^{-7} **(22)**
1.3×10^{-8} **(5)**	5.6×10^{-8} **(11)**	3.0×10^{-7} **(17)**	4.3×10^{-7} **(23)**
1.6×10^{-8} **(6)**	5.9×10^{-8} **(12)**	3.1×10^{-7} **(18)**	

ment. The probing wave—having a constant input force—is in the same amplitude range for every conditioning strain. Therefore, the difference in nonlinearity between different conditioning strain levels is negligible. The short recovery times enable a high sensitivity in the measurements of low strain levels which removes the shortcoming of the previous method B. The conditioning strain levels are found in table, the last one is a factor 640 higher than the lowest value. The probe strain level is below the smallest conditioning level which is 6.7×10^{-10}.

The resonance frequencies for the 23 strain curves as a function of time after end of conditioning (τ_l) are shown in Fig. 6. There is a trend of decrease in resonance frequency (or wave speed) with increase in conditioning strain for curves (*14–23*).

The curves would probably for long enough times approach a limit value irrespective of the conditioning level. The reason why we did not use longer times τ, for example 10 minutes, is that the test would have taken a much longer time. A 10-minute recovery time test would take about one year, if performed perfectly. However, it would not be long enough to reach the limit of the process. The 23 valued 0.2–5-second test in this article took about 6 weeks of round the clock measurements.

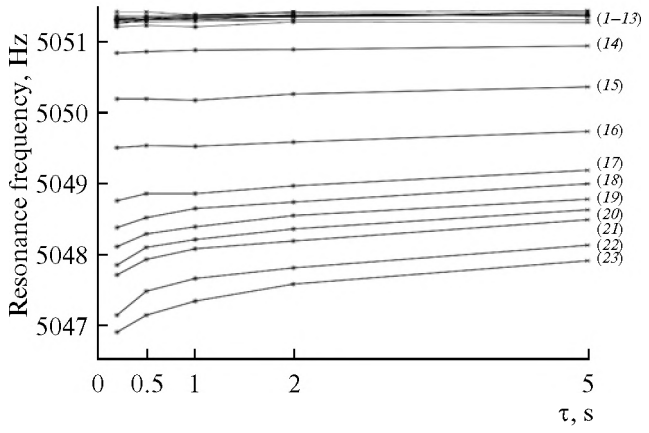

Fig. 6. The early time evolution of Slow Dynamics for the strain region: 6.7×10^{-10}–4.3×10^{-7}. The low strains between 6.7×10^{-10} and 6.2×10^{-8} are collected in the top bundle, and the higher strains are below in order.

It is difficult to find a function which fits the time evolution of all the curves. An obvious trend—for the strains above 2×10^{-8}—is that the resonance frequency increases with time (τ) when letting the material recover. Also the recovery speed (i.e. the slope) is higher for larger resonance frequency shifts, which is to be expected.

Figure 7 shows the resonance frequency curves for the five values as functions of the conditioning strain. The curves represents the points taken at $\tau_l = 0.2$, 0.5, 1, 2, and 5 seconds after end of conditioning. This displays how the resonance frequency—and wave speed—is first increasing, and thereafter decreases steadily. To confirm this a different accelerometer (a PCB 352A25) was used in another test whose result is presented in Fig. 8. The whole measurement procedure was repeated, starting with the two week rest in the climate chamber, and the number of conditioning strains were now 7 (instead of 23), ranging from 6.7×10^{-10}–3.3×10^{-8} (a factor of about 50). The accelerometer mass was added to the system so the initial resonance frequency was changed slightly, but this did not qualitatively affect the response.

For strains above $\epsilon_C = 0.06$ με ($\ll \epsilon_P < 6.7 \times 10^{-10}$) the dependence of sound velocity on strain is decreasing close to linearly. For the strains below this value the sound velocity increases with strain. In general the measurement points in Figs. 7 and 8 are in order with increasing recovery time τ_l. It is noteworthy to see that even at the lowest strain, there is an ordered difference between the curves, which indicates that a slow dynamic recovery effect exists even in this regime. In other words, no threshold value for the Slow Dynamics effect was found, and the process seem to consist of two competing processes. One is stronger for lower strains and stiffens the rock (increasing the resonance frequency), while the other is dominating at higher strains and weakens the rock (lowering the resonance frequencies). First the increase of resonance frequency takes place until 1.6×10^{-8} which has the maximum for all the curves. After this the curves turn down before a second, slightly lower, maximum is found at around 6×10^{-8}. Then a decrease is starting, which continues for all the higher values.

This is the first test that really monitors (a) the material state at a given strain; and (b) the pure recovery process (from that given state). These results are influenced neither by the nonlinearity nor by the pre-

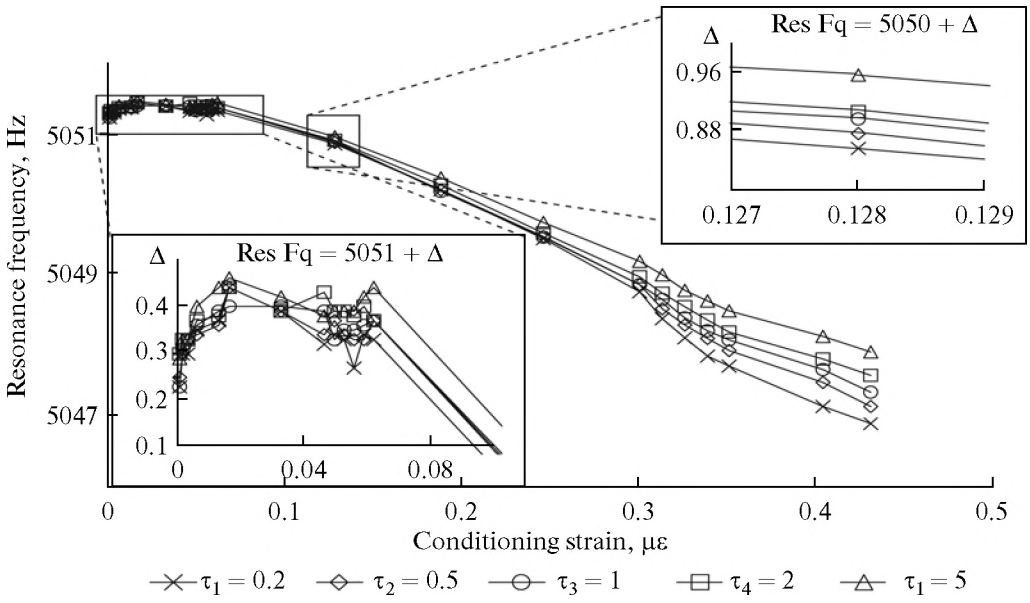

Fig. 7. The resonance frequency as a function of conditioning strains ε_C for the five recovery times $\tau_l = 0.2$, 0.5, 1, 2 and 5 s.

vious time history. For the first time the relevant recovery starting time can be defined (at $\tau = 0$). I.e. a new method has been presented which is the first that measures purely the Slow Dynamics property of a material.

Above the region around 0.015–0.06 με the behavior is more or less linearly decreasing on strain. Below, the limiting behavior is still inconclusive—in our tests it is decreasing for the lowest strains. Is this a *general* behavior? Will it be repeated for other rocks and for other materials? With this method it is possible to investigate this in a consistent way.

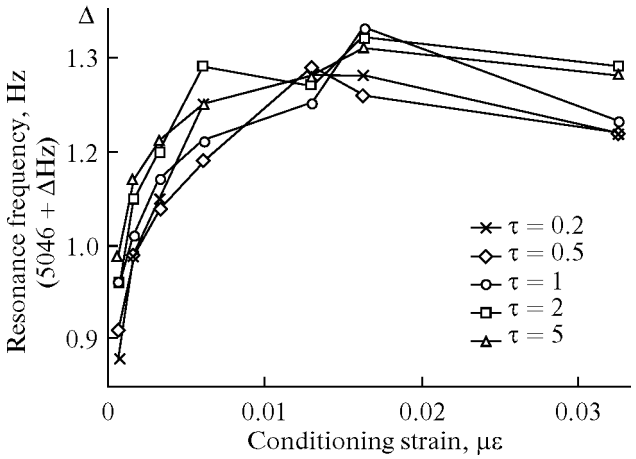

Fig. 8. The resonance frequency measured with a different accelerometer shows the same behavior as in Fig. 7.

ACKNOWLEDGMENTS

This work is financed by VINNOVA, and the KK Foundation, Sweden. R.A. Guyer is gratefully acknowledged for interesting discussions and viewpoints.

REFERENCES

1. V. A. Robsman, Akust. Zh. **39**, 333 (1993).
2. P. A. Guyer and P. A. Johnson, Phys. Today **52**, 30 (1999).
3. J. A. TenCate, E. Smith, and P. A. Guyer, Phys. Rev. Lett. **85**. 1020 (2000).
4. G. Zaitsev, G. Gusev, and B. Castagnede, Phys. Rev. Lett. **90**, 075501 (2003).
5. A. B. Nazarov, A. B. Kolpakov, and A. V. Radostin, Acoust. Phys. **55**, 100 (2009).
6. R. A. Guyer and P. A. Johnson, *Nonlinear Mesoscopic Elasticity: The Complex Behavior of Rocks, Soils, Concrete* (Wiley, 2009).
7. K. C. E. Haller, C. M. Hedberg, and O. V. Rudenko, Acoust. Phys. **56**, 660 (2010).
8. O. V. Rudenko, A. I. Korobov, and M. Yu. Izosimova, Acoust. Phys. **56**, 151 (2010).
9. C. M. Hedberg and O. V. Rudenko, J. Appl. Phys. **110**, 053503 (2011).
10. J. A. TenCate and T. J. Shankland, Geophys. Res. Lett. **23**, 3019 (1996).
11. J. A. TenCate, D. Pasqualini, S. Habib, K. Heitmann, D. Higdon, and P. A. Johnson, Phys. Rev. Lett. **93**, 065501 (2004).
12. D. Pasqualini, K. Heitmann, J. A. TenCate, S. Habib, and D. Higdon, J. Geophys. Res. B **112**, 01204 (2007).
13. K. C. E. Haller and C. M. Hedberg, Phys. Rev. Lett. **100**, 068501 (2008).
14. R. A. Guyer, J. A. TenCate, and P. A. Johnson, Phys. Rev. Lett. **82**, 3280 (1999).
15. S. Stanchits, S. Vinciguerra, and G. Dresen, Pure Appl. Geophys. **163**, 974 (2006).